Neurobiology of Disease 88 (2016) 44–54

Contents lists available at ScienceDirect

Neurobiology of Disease

journal homepage: www.elsevier.com/locate/ynbdi

Long-term controlled GDNF over-expression reduces dopamine transporter activity without affecting tyrosine hydroxylase expression in the rat mesostriatal system

Pedro Barroso-Chinea [a], Ignacio Cruz-Muros [a], Domingo Afonso-Oramas [a], Javier Castro-Hernández [a], Josmar Salas-Hernández [a], Abdelwahed Chtarto [b], Diego Luis-Ravelo [a], Marie Humbert-Claude [c], Liliane Tenenbaum [c], Tomás González-Hernández [a,d,*]

[a] Departamento de Ciencias Médicas Básicas (Anatomía), Facultad de Ciencias de la Salud (Medicina), Instituto de Tecnologías Biomédicas (ITB, CIBICAN), Universidad de La Laguna, Tenerife, Spain
[b] Laboratory of Experimental Neurosurgery and Multidisciplinary Research Institute (I.R.I.B.H.M.), Free University of Brussels (ULB), Brussels, Belgium
[c] Laboratory of Cellular and Molecular Neurotherapies, Neuroscience Research Center, Department of Clinical Neuroscience, Lausanne University Hospital, Switzerland
[d] Centro de investigación Biomédica en Red sobre enfermedades neurodegenerativas, CIBERNED, Instituto de Salud Carlos III, Spain

ARTICLE INFO

Article history:
Received 9 September 2015
Revised 7 December 2015
Accepted 7 January 2016
Available online 9 January 2016

Keywords:
Dopamine transporter
Tyrosine hydroxylase
GDNF
Inducible adeno-associated viral vectors
Parkinson's disease

ABSTRACT

The dopamine (DA) transporter (DAT) is a plasma membrane glycoprotein expressed in dopaminergic (DA-) cells that takes back DA into presynaptic neurons after its release. DAT dysfunction has been involved in different neuro-psychiatric disorders including Parkinson's disease (PD). On the other hand, numerous studies support that the glial cell line-derived neurotrophic factor (GDNF) has a protective effect on DA-cells. However, studies in rodents show that prolonged GDNF over-expression may cause a tyrosine hydroxylase (TH, the limiting enzyme in DA synthesis) decline. The evidence of TH down-regulation suggests that another player in DA handling, DAT, may also be regulated by prolonged GDNF over-expression, and the possibility that this effect is induced at GDNF expression levels lower than those inducing TH down-regulation. This issue was investigated here using intrastriatal injections of a tetracycline-inducible adeno-associated viral vector expressing human GDNF cDNA (AAV-tetON-GDNF) in rats, and doxycycline (DOX; 0.01, 0.03, 0.5 and 3 mg/ml) in the drinking water during 5 weeks. We found that 3 mg/ml DOX promotes an increase in striatal GDNF expression of 12× basal GDNF levels and both DA uptake decrease and TH down-regulation in its native and Ser40 phosphorylated forms. However, 0.5 mg/ml DOX promotes a GDNF expression increase of 3× basal GDNF levels with DA uptake decrease but not TH down-regulation. The use of western-blot under non-reducing conditions, co-immunoprecipitation and *in situ* proximity ligation assay revealed that the DA uptake decrease is associated with the formation of DAT dimers and an increase in DAT–α-synuclein interactions, without changes in total DAT levels or its compartmental distribution. In conclusion, at appropriate GDNF transduction levels, DA uptake is regulated through DAT protein–protein interactions without interfering with DA synthesis.

1. Introduction

The uptake of dopamine (DA) into presynaptic terminals is the primary mechanism controlling the duration and intensity of DA signaling in post- and presynaptic DA receptors (Giros et al., 1996). The DA transporter (DAT) is a plasma membrane glycoprotein expressed in dopaminergic (DA-) cells, responsible for DA uptake through a Na^+/Cl^- coupled cotransport mechanism (Giros and Caron, 1993; Freed et al., 1995). DAT dysfunction has been involved in a number of neuro-psychiatric disorders, including Parkinson's disease (PD) (Le Couteur et al., 1997; Bezard et al., 1999; Zahniser and Sorkin, 2009; Storch et al., 2004). Taking into account that oxidative stress plays a central role in the pathogenesis of PD, that DA metabolism is the main source of reactive oxygen species in DA-cells, and that the cytosolic content in DA depends mostly on the DA uptake (Bannon, 2005), DAT activity has been involved in DA-cell degeneration in PD. This idea is supported on the fact that midbrain DA-cells showing high susceptibility to degeneration contain higher levels of DAT mRNA and glycosylated (functional) DAT protein than those showing resistance (Uhl et al., 1994; Afonso-Oramas et al., 2009). Moreover, DAT transports natural and synthetic DA analog neurotoxins, and its blockade or deficient expression makes DA-cells resistant to these neurotoxins (Bezard et al., 1999; Schober, 2004; Gonzalez-Hernandez et al., 2004; Afonso-Oramas et al., 2010).

* Corresponding author at: Departamento de Ciencias Médicas Básicas (Anatomía), Facultad de Ciencias de la Salud (Medicina), Universidad de La Laguna, 38207 La Laguna, Tenerife, Spain.
E-mail address: tgonhern@ull.es (T. González-Hernández).
Available online on ScienceDirect (www.sciencedirect.com).

http://dx.doi.org/10.1016/j.nbd.2016.01.002
0969-9961/

DAT is acutely regulated by different factors including extracellular DA levels, DA autoreceptors, and interactions with presynaptic proteins such as α-synuclein, protein kinases and phosphatases which promote either its trafficking to the plasma membrane and activity or its internalization (Mortensen and Amara, 2003; Wersinger and Sidhu, 2003; Miranda and Sorkin, 2007; Eriksen et al., 2010a, 2010b; Foster et al., 2012). On the other hand, phenotypic and functional properties of DA-cells, including DA transport, are maintained by different neurotrophic factors (Alexi et al., 2000; Pascual et al., 2008; Apawu et al., 2013). Particular interest has been focused on the glial cell line-derived neurotrophic factor (GDNF). *In vitro* and *in vivo* experiments show that besides protecting DA-cells against different neurotoxins (Kirik et al., 2004; Garbayo et al., 2011), GDNF promotes tyrosine hydroxylase (TH, the limiting enzyme in DA synthesis) expression and DA release, turnover and uptake (Lin et al., 1993; Salvatore et al., 2004; Yang et al., 2009). Based on these findings, GDNF was proposed as a hopeful neuroprotective therapy in PD. However, further studies in rodents revealed that prolonged GDNF release may lead to TH down-regulation (Rosenblad et al., 2003; Georgievska et al., 2004), probably as a consequence of the elevated DA turnover induced by excessive GDNF overexpression (Rosenblad et al., 2003; Sajadi et al., 2005). So, it is possible that other players in DA handling are affected by sustained GDNF treatment. Given the role of DAT in DA handling and in the pathogenesis of PD, here we investigated whether DAT is also regulated by prolonged GDNF treatment, and more important, if DAT may be regulated without affecting TH expression. Taking advantage of the fact that regulatable viral vectors allow a fine control of target gene expression through external inducers (Goverdhana et al., 2005; Chtarto et al., 2013), experiments here were based on intrastriatal injections of a tetracycline-inducible adeno-associated viral vector expressing human GDNF cDNA and treatment with different doses of doxycycline in rats.

2. Material and methods

2.1. Plasmids

The pAC1-M2 plasmid comprising AAV ITRs bracketing the bidirectional tetracycline-responsive cassette expressing both rtTAM2 and EGFP has been previously described (Chtarto et al., 2007). To obtain pAC1-V16, the rtTA transactivator of pAC1 was replaced by rtTAV16, a rtTA mutant selected in the presence of a low doxycycline dose (Zhou et al., 2006). The human GDNF cDNA (hGDNF) was introduced in this autoregulatory tetracycline inducible vector at the 5′ end of the bidirectional tetracycline promoter ($ptet_{bidi}ON$).

2.2. Viral production

To produce recombinant AAV2/1 viral stocks, HEK-293T cells (5.0×10^6 cells per 10 cm plates) were cotransfected, in a 1:1 molar ratio, with the vector plasmid (3 μg/plate) together with the helper/packaging plasmid pD1rs (10 μg/plate) expressing the AAV viral genes (rep gene from AAV serotype 2 and cap gene from AAV serotype 1) and the adenoviral genes required for AAV replication and encapsidation (Plasmid Factory, Heidelberg, Germany). Fifty hours post-transfection, the medium was discarded and the cells were harvested by low-speed centrifugation and resuspended in Tris pH 8.0, NaCl 0.1 M. After three cycles of freezing/thawing, the lysate was clarified by 30 min centrifugation at 10,000 *g*, treated with benzonase (50 units/ml, Sigma, St Louis, MO) at 37 °C for 30 min, and centrifuged at 10,000 *g* for 30 min to eliminate the residual debris. The virus was further purified by iodixanol gradient according to a well-established method (Zolotukhin et al., 2002). Viral genomes (vg) were titrated by quantitative PCR as previously described (Lock et al., 2010).

2.3. Animals

The experiments were carried out on male Sprague–Dawley rats (300–350 g; Charles River, France). Rats were housed in groups of 3–4 per cage, in conditions of constant temperature (21–22 °C), a 12 h light/dark cycle, and given free access to food and water. Experimental protocols were approved by the Ethical Committee of the University of La Laguna (reference # 091/010), and are in accordance with the European Communities Council Directive of 22 September 2010 (2010/63/EU) regarding the care and use of animals for scientific purposes.

Stereotaxic injections (David Kopf Instruments, Tujunga, CA) were performed under ketamine (Imalgene®; 100 mg/kg, i.p.) and xylazine (Rompun®; 45 mg/kg, i.p.) anesthesia using a syringe (Hamilton 701N, Reno, NV) with a 26S gauge blunt-tip needle. Rats received 3 μl of a viral suspension of recombinant AAV2/1-V16-hGDNF ($n = 18$) or AAV2/1-V16-EGFP ($n = 14$), or vehicle (Dulbecco's phosphate-buffered saline; BioWhittaker, Walkersville, MD, USA; $n = 14$) in the left striatum. Viral suspension (3.5×10^{11} vg/ml) and vehicle were delivered in two deposits (1.5 μl each) 0.7 mm apart along the same needle tract at a diffusion rate of 0.5 μl/min at the following coordinates: 0.5 mm rostral to bregma, 2.6 mm lateral to midline, and 5.2 mm (first deposit) and 4.5 mm (second deposit) ventral from the skull surface (Paxinos and Watson, 1998). After injection, the needle was left in place for 5 min to allow diffusion of the viral suspension in the parenchyma and then slowly removed. Viral vector injected rats were treated with doxycycline (DOX) in the drinking water containing 3% sucrose at a concentration of 0.01, 0.03, 0.5 and 3 mg/ml since the injection day to the sacrifice. Animals were sacrificed by an overdose of sodium pentobarbital at 5 weeks after injection and the brains were removed and processed for morphological and biochemical analysis. A group of rats receiving 3 mg/ml DOX was maintained without DOX treatment for 20 additional days before sacrifice. Experimental groups included at least 5 rats in each experiment.

2.4. DAT antibodies

Several commercial anti-DAT antibodies against different fragments of human and rat DAT have been tested in our laboratory to determine their specificity and sensitivity. Brain samples of different mammalians and cells transfected with wild type and mutated DAT forms were processed for immunohistochemistry, western-blot and immunoprecipitation (see Afonso-Oramas et al., 2009, 2010; Cruz-Muros et al., 2009). Taking into account the results of these tests, a goat anti-DAT polyclonal antibody (Santa Cruz Biotechnology, Santa Cruz, CA) was used for western-blot, and a rabbit anti-DAT polyclonal antibody (Millipore, Billerica, MA) for immunoprecipitation. For the study of DAT–DAT interaction using *in situ* proximity ligation assays, the goat anti-DAT polyclonal antibody was combined with a rabbit anti-DAT polyclonal antibody (Santa Cruz Biotechnology, Santa Cruz, CA).

2.5. GDNF immunohistochemistry

Animals were transcardially perfused with heparinized ice-cold 0.9% saline followed by 4% paraformaldehyde in PBS, pH 7.4. The brains were removed, and the midbrain and forebrain blocks were stored in the same fixative at 4 °C overnight, cryoprotected in a graded series of sucrose–PBS solutions, and stored at −80 °C until processing. Coronal sections (30 μm) were obtained with a freezing microtome and collected in 6–8 parallel series. Floating sections were immersed for 30 min in 3% H_2O_2 to inactivate endogenous peroxidase, and incubated for 60 min at RT in 4% normal donkey serum (NDS, Jackson ImmunoResearch, West Grove, PA) in PBS, containing 0.05% Triton X-100 (TX-100, Sigma), and overnight in PBS containing 2% NDS and a goat anti-GDNF polyclonal antibody (1:500; R&D Systems, Minneapolis, MN). After several rinses, sections were incubated for 2 h in biotinylated donkey anti-goat

antiserum (1:1000, Jackson ImmunoResearch) and 1:200 NDS in PBS. Immunoreactions were visible after incubation for 1 h at RT in ExtrAvidin-peroxidase (1:5000, Sigma) in PBS, and after 10 min in 0.005% 3′,3′-diamiobenzidine tetrahydrochloride (DAB, Sigma) and 0.001% H_2O_2 in cacodylate buffer 0.05 N pH 7.6.

2.6. In situ proximity ligation assay (PLA)

This technique is based on the use of oligonucleotide-conjugated antibodies, ligation of oligonucleotides by a bridging probe in a proximity-dependent manner, rolling-circle amplification, and visualization by complementary fluorescent probes (Söderberg et al., 2008). DAT–DAT interaction and DAT interactions with D_2R and α-synuclein were studied using the Duolink II *in situ* PLA detection kit (Sigma) as described by Castro-Hernández et al. (2015). Briefly, for the study of DAT–D_2R and DAT–α-synuclein interactions, sections were incubated overnight at 4 °C with a goat polyclonal anti-DAT antibody (1:200; Santa Cruz Biotechnology) and one of the following antibodies in the antibody diluent: rabbit polyclonal anti-D_2R antibody (1:200; Millipore) or rabbit polyclonal anti-α-synuclein antibody (1:200, Santa Cruz Biotechnology). Thereafter, sections were incubated (2 h, 37 °C) with PLA probes detecting goat and rabbit antibodies (Duolink II plus PLA probe anti-goat and Duolink II minus PLA probe anti-rabbit) and processed for ligation, amplification, and detection as described by the manufacturer. For the study of DAT–DAT interactions, sections were incubated with two anti-DAT antibodies directed to the C-terminus (1:200 rabbit polyclonal anti-DAT and 1:200 goat-polyclonal anti-DAT) and PLA probes detecting rabbit (plus) and goat (minus) antibodies. For negative controls, one of the primary antibodies was substituted by non-immune goat or rabbit IgG, resulting in negative staining. Some sections were additionally processed for tyrosine hydroxylase (TH, the rate-limiting enzyme in DA synthesis) immunofluorescence by using a mouse monoclonal anti-TH antibody (1:4000, Sigma). To avoid autofluorescence caused by the presence of fluorescent pigments such as lipofucsin or elastin and also by the fixative, sections were treated with $CuSO_4$ in ammonium acetate buffer (5 mM $CuSO_4$, 50 mM ammonium acetate pH 5.0) for 10 s (Zieba et al., 2010). After several washes they were mounted in mounting medium with DAPI and examined under a confocal laser scanning microscopy system (Olympus FV1000, Hamburg, Germany). Images were acquired in Z-stack mode (8.5 μm total thickness, 4 z-steps). Fluorescent PLA point-like signals were quantified, in number and size, in at least 12 striatal regions (400 μm × 400 μm) from 5 different rats per experimental group for each pair of primary antibodies, by using the ImageJ standard program.

2.7. Striatal GDNF determination by enzyme-linked immunosorbent assay (ELISA)

Five weeks after injection, rats (n = 5 in each experimental group) were sacrificed and left striata were dissected in ice from freshly obtained brains using a brain blocker. The samples were sonicated in homogenization buffer (137 mM NaCl, 20 mM Tris (pH 8.0), 1% NP40, 10% glicerol, 1 mM PMSF, 10 μg/ml aprotinin, 1 μg/ml leupeptin and 0.5 mM sodium vanadat) and striatal GDNF levels were determined by ELISA test following the manufacturer's guidelines (commercial kit G7620, Promega Corporation, Madison, WI). Data are expressed as picograms of GDNF per milligram of total proteins.

2.8. Synaptosomal [^{3}H]-DA uptake

Rat striata were obtained as described for GDNF ELISA, and processed according to Afonso-Oramas et al. (2009). Samples were immediately homogenized in 20 vol of ice-cold sucrose bicarbonate solution (SBS, 320 mM sucrose in 5 mM sodium bicarbonate, pH 7.4) with 12 up and down strokes in a Teflon-glass homogenizer. The homogenates were centrifuged (1000 ×*g*, 10 min, 4 °C), and the pellets (P1) containing nuclei and large debris discarded. The supernatants (S1) were centrifuged (17,000 ×*g*, 20 min, 4 °C), and the pellets (P2) were resuspended in 500 μl ice-cold assay buffer (125 mM NaCl, 5 mM KCl, 1.5 mM $MgSO_4$, 1.25 mM $CaCl_2$, 1.5 mM KH_2PO_2, 10 mM glucose, 25 mM HEPES, 0.1 mM EDTA, 0.1 mM pargyline and 0.1 mM ascorbic acid). For [^{3}H]-DA uptake assays, a range of temperatures (25–35 °C), DA concentrations (20–500 nM), incubation times (5–30 min) and striatal protein concentrations (0.2–3 μg/μl) were checked in order to establish the working parameters in the linear ascending segment of the uptake curve. Fifty microliters of synaptosomal suspension (0.5 μg total protein/μl) was preincubated with 50 nM DA (Sigma) with or without 10 μM nomifensine (Sigma) in assay buffer (30 °C, 5 min). Subsequently, 20 nM [^{3}H]-DA (final concentration; Amersham, Buckinghamshire, UK) was added to each tube. The total assay volume was 200 μl. After 10 min incubation at 30 °C, DA uptake was stopped by the addition of 200 μl ice-cold assay buffer. The suspension was immediately filtered under vacuum through MultiScreen®-0.45 μm hydrophilic filters (Millipore, Molsheim, France). The filters were washed twice with 200 μl ice-cold assay buffer, excised and placed in scintillation vials containing 3 ml liquid scintillation Cocktail (Sigma), and stored overnight at room temperature (RT). Accumulated radioactivity was quantified using a liquid scintillation counter (LKB Rackbeta 1214; Turku, Finland). Non-specific uptake, defined as the DA uptake in the presence of nomifensine, was subtracted from total uptake to define DAT-mediated specific uptake. All assays were performed in triplicate.

2.9. Western-blot in whole striatal extracts and plasma membranes

DAT expression was studied using western-blot analysis of total extracts and the plasma membrane fraction of striatal synaptosomes. The striata were dissected as described for DA uptake. Whole protein extracts were obtained using the acid phenol method, resuspended in radioimmunoprecipitation assay (RIPA) lysis buffer pH 7.4 containing protease and phosphatase inhibitor cocktails (Roche Diagnostics, Indianapolis, IN), and quantified using the bicinchoninic acid method and bovine serum albumin as standard. Plasma membranes were obtained following the impermeant biotynilation procedure (Salvatore et al., 2003). Synaptosomes (300 μg total protein) were incubated for 1 h at 4 °C with continual shaking in 500 μl of 1.5 mg/ml sulfo-NHS-biotin (Pierce, Rockford, IL) in PBS/Ca/Mg buffer (138 mM NaCl, 2.7 mM KCl, 1.5 mM KH_2PO_2, 9.6 mM Na_2HPO_4, 1 mM $MgCl_2$, 0.1 mM $CaCl_2$, pH 7.3) and centrifuged (8000 ×*g*, 4 min, 4 °C). In order to remove biotinylating reagents, the resulting pellets were resuspended in 1 ml ice-cold 100 mM glycine in PBS/Ca/Mg buffer and centrifuged (8000 ×*g*, 4 min, 4 °C). The resuspension and centrifugation steps were repeated. Final pellets were resuspended again in 1 ml ice-cold 100 mM glycine in PBS/Ca/Mg buffer and incubated for 30 min at 4 °C. Samples were washed three more times in PBS/Ca/Mg buffer, and then lysed by sonication for 2–4 s in 300 μl Triton X-100 buffer (10 mM Tris, pH 7.4, 150 mM NaCl, 1 mM EDTA, 1% Triton X-100) containing protease and phosphatase inhibitor cocktails (Roche Diagnostics). After incubation in continuous shaking (30 min, 4 °C), the lysates were centrifuged (18,000 ×*g*, 30 min, 4 °C), and the supernatants were incubated with monomeric avidin bead-Triton X-100 buffer (100 μl) for 1 h at RT, and centrifuged (18,000 ×*g*, 4 min, 4 °C). The resulting pellets (containing avidin-absorbed biotynilated surface proteins) were resuspended in 1 ml Triton X-100 buffer and centrifuged (18,000 ×*g*, 4 min, 4 °C). Resuspension and centrifugation were repeated two more times, and the final pellets were stored.

Protein samples for western-blot analysis were diluted in Laemmli's loading buffer (62.5 mM Tris–HCl, 20% glycerol, 2% sodium dodecyl sulfate [SDS; Sigma], 1.7% β-mercaptoethanol and 0.05% bromophenol blue, pH 6.8), denatured (90 °C, 1 min), separated by electrophoresis in 10% SDS-polyacrylamide gel, and transferred to nitrocellulose (Schleicher & Schuell, Dassel, Germany). Blots were blocked for 2 h at

RT with 5% non-fat dry milk in TBST (250 mM NaCl, 50 mM Tris, pH 7.4, and 0.05% Tween20), and incubated overnight at 4 °C in blocking solution with one of the following primary antibodies: a goat polyclonal anti-DAT antibody (1:500, Santa Cruz Biotechnology), a mouse monoclonal antibody that recognized native tyrosine hydroxylase (TH; Sigma; 1:10,000, overnight, 4 °C), a rabbit polyclonal antibody recognizing rat TH amino acids residues surrounding the phospho-serine 40 (THp40; PhosphoSolutions, Aurora, CO; 1:1000, overnight, 4 °C) and a mouse anti-β-actin antibody (Sigma,1:10,000, 2 h, RT). After several rinses in TBST-5% milk, the membranes were incubated for 1 h in horseradish peroxidase conjugated anti-goat (1:5000), anti-rabbit (1:10,000) or anti-mouse (1:20,000) IgG (Jackson-ImmunoResearch). In western blot for the THp40, milk was substituted by 5% bovine serum albumin in the blocking solution. Immunoreactive bands were visualized using enhanced chemiluminiscence (Immun-Star, Bio-Rad, CA) and a Chemi-Doc™ XRS imaging system (Bio-Rad, Hercules, CA).

Different protein quantities, antibody dilutions and exposure times were tested to establish the working range of each antibody. The labeling densities for DAT, TH and THp40 were compared with β-actin by using densitometry software (Bio-Rad). A rectangle of uniform size and shape was placed over each band, and the density values were calculated by subtracting the background at approximately 2 mm above each band. The effectiveness of the plasma membrane fractionation was evaluated by using Syntaxin (mouse monoclonal anti-syntaxin, 1:500, Sigma) as a marker of synaptosomal membrane.

2.10. Western-blot analysis under non-reducing conditions

Western-blot analysis under non-reducing conditions was performed according to Baucum et al. (2004). Briefly, synaptosomes were obtained as described for DA uptake using 0.32 M sucrose, supplemented with protease inhibitor cocktail and PhosStop phosphatase inhibitor cocktail (Roche Diagnostics) and 10 mM N-ethylmaleimide (NEM; Sigma) as homogenization solution. P2 pellets were resuspended in Milli-Q water, protein concentration was quantified, and samples were mixed with loading buffer (2.25% SDS, 18% glycerol, 180 mM Tris base, pH 6.8, and bromophenol blue). Fifteen micrograms of total protein was loaded into each well, separated by electrophoresis in 9% SDS-polyacrylamide gel containing 0.1% SDS, and transferred to nitrocellulose (Schleicher & Schuell). DAT immunostaining and quantification were performed as described above.

2.11. Co-immunoprecipitation

Co-immunoprecipitation was performed according to HadlocK et al. (2011) with minor modifications. Striatal tissue was homogenized in 1.5 ml ice-cold 10 mM HEPES, 0.32 M sucrose and 10 mM NEM pH 7.4, and centrifuged (800 ×*g*, 12 min, 4 °C). The supernatants (S1) were centrifuged at 22,000 ×*g*, 15 min, 4 °C, and the resulting pellets (P2) resuspended in 100 μl M-PER (Thermo Scientific, Rockford, IL). After 1 h at 4 °C in gentle shaking, samples were centrifuged again, the pellets were discarded, and protein concentration was quantified in supernatants. Aliquots of 500 μg proteins were incubated in protein A-Sepharose beads (100 μl stock suspension in 200 μl M-PER; 4 °C, 45 min) to pre-clear endogenous immunoglobulins. After gentle centrifugation, pre-cleared supernatants were incubated with anti-DAT, anti-D2R or non-immune IgG overnight at 4 °C in continuous shaking. In the experience of this laboratory, the most robust immunoprecipitates are obtained using 6 μl of rabbit polyclonal anti-DAT from Millipore®, rabbit polyclonal anti-D_2R from Millipore®. Protein A-Sepharose beads (100 μl stock suspension in 200 μl M-PER) were added and maintained in continuous shaking at 4 °C for 3 h. Immuno-complexes were precipitated by gentle centrifugation. After extensive washing, they were resuspended in 40 μl Laemmli's buffer, denatured, separated by electrophoresis in 10% SDS-polyacrylamide gel and transferred to nitrocellulose. Blots from DAT precipitates were immunoreacted for α-synuclein and DAT using a mouse monoclonal anti-α-synuclein (1: 500, BD Biosciences, San Jose, CA) and a goat polyclonal anti-DAT antibody (1:500, Santa Cruz Biotechnology). Blots from D_2R precipitates were immunoreacted for DAT and D_2R using a goat anti-DAT polyclonal (1:500, Santa Cruz Biotechnology) and a mouse monoclonal anti-D_2R antibody (1:500, Santa Cruz Biotechnology).

2.12. Statistics

Mathematical analysis was performed using the one way ANOVA followed by the Tukey honest test for multiple post hoc comparisons. Analysis was performed using the Statistica program (Statsoft; Tulsa, U.S.A.). The degree of freedom in all comparisons was 1 (intergroup) and 8 (intragroup). A level of $p < 0.01$ was considered as critical for assigning statistical significance. Data are expressed as mean ± standard error of the mean.

3. Results

3.1. Regulated GDNF over-expression promotes DA uptake decrease without changes in DAT and TH expression.

To determine the effect of different GDNF transduction levels on DAT and TH, viral vector injected rats were treated with doxycycline (DOX) for 5 weeks. DOX was administered in the drinking water at a concentration of 0.01, 0.03, 0.5 and 3 mg/ml. The daily drinking volume stabilized two days after GDNF injection at 57 ± 3 ml. As shown in Fig. 1A, striatal levels of GDNF in AAV-tetON-GDNF injected rats receiving 0.01 and 0.03 mg/ml DOX were similar to those in AAV-tetON-GFP injected rats receiving 0.01 and 3 mg/ml DOX, and sham injected untreated rats. In AAV-tetON-GDNF injected rats receiving 0.5 mg/ml DOX, GDNF transduction tripled the basal levels (69.3 ± 3.6 *vs.* 22.6 ± 5.2 pg/mg protein, $p < 0.01$; $F = 12.18$), and sparse neurons became immunoreactive for GDNF in the injection place (Fig. 1F, G). In rats receiving 3 mg/ml DOX, GDNF levels were 12 times higher (253.3 ± 7.9 pg/mg protein; $p < 0.001$; $F = 9.26$) than in AAV-tetON-GFP-injected rats, and many neurons became intensely immunoreactive for GDNF around the injection place (Fig. 1 H, I).

Western-blot analysis of TH expression (Fig. 2A) revealed that, consistent with previous reports (Rosenblad et al., 2003; Georgievska et al., 2004), the levels of TH, in its native form, are decreased in striata with 12× basal GDNF over-expression (3 mg/ml DOX; 53%; $p < 0.01$, $F = 6.31$). However, no changes were detected in those with 3× basal GDNF over-expression (0.5 mg/ml DOX). TH phosphorylated at the Ser40 residue (THp40) followed the same pattern as the native form, with a decrease at 12× GDNF over-expression (80%; $p < 0.01$; $F = 12.48$) but no changes at 3× GDNF overexpression. By contrast, the analysis of DAT expression in whole striatal extracts and in the plasma membrane of striatal terminals (Fig. 2B) revealed no differences between both experimental conditions,12× and 3× GDNF over-expression, and sham-injected rats. However, the analysis of nomifensine-sensitive DA uptake in striatal synaptosomes (Fig. 2C) revealed a significant DA uptake decrease in both 0.5 mg/ml DOX-(44.8 ± 4.1%, $p < 0.01$; $F = 12.73$) and 3 mg/ml DOX-treated rats (49.6 ± 3.3%; $p < 0.01$; $F = 12.75$) with respect to sham-injected rats. In addition, after 20 days without DOX, DA uptake returned to normal levels. These data indicate that sustained GDNF over-expression induces a DA uptake decrease without changes in the expression levels and subcellular distribution of DAT, and more interestingly, that a 3× increase in GDNF delivery reduces DA uptake without affecting TH expression.

3.2. Prolonged GDNF over-expression induces the formation of DAT dimers and DAT–α-synuclein interactions.

The finding of a decrease in DA uptake but not in DAT levels in whole striatal extracts or synaptosomal membranes suggests that the effect of

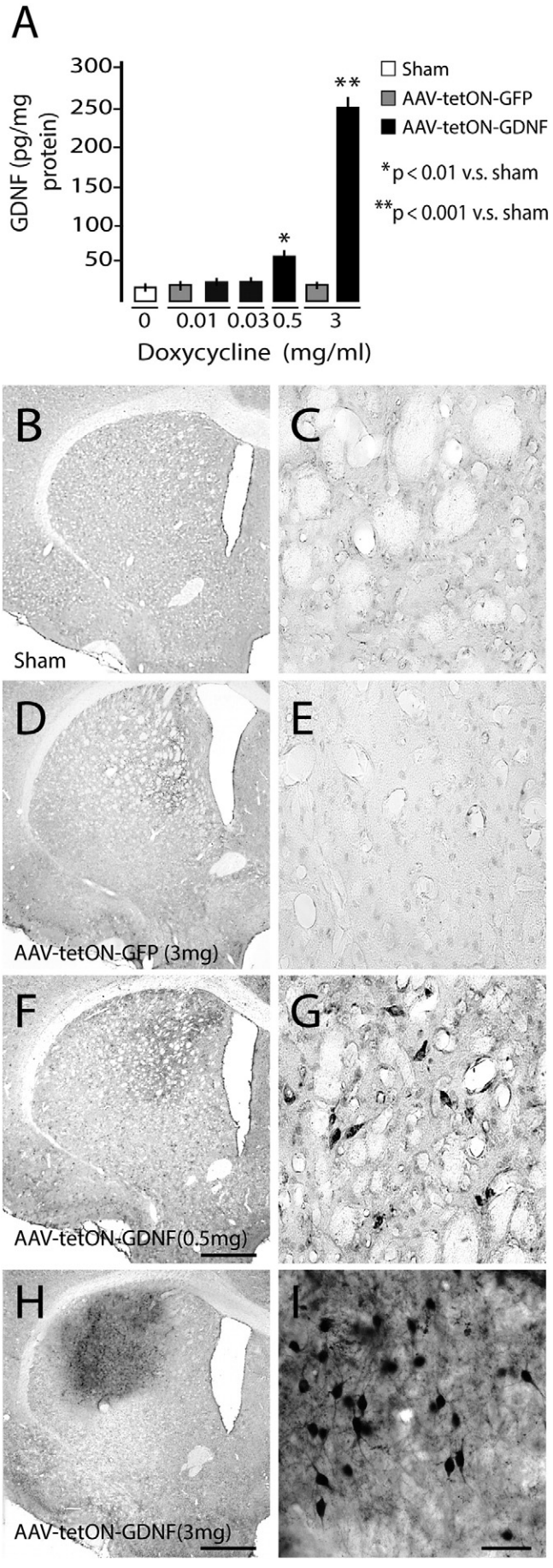

prolonged GDNF over-expression on DA uptake is not mediated by DAT expression down-regulation or internalization. Although trafficking between the plasma membrane and intracellular compartments and lysosomal degradation are considered the standard mechanisms of DAT regulation (Mortensen and Amara, 2003; Eriksen et al., 2010b; Gabriel et al., 2013), we know that transporters may form complexes with themselves (Hastrup et al., 2001; Torres et al., 2003; Baucum et al., 2004) and other presynaptic proteins which regulate transporter activity (González and Robinson, 2004; Chen and Reith, 2008; Eriksen et al., 2010b). Thus, possible changes in DAT–DAT and DAT interactions with two well-known members of its proteome, α-synuclein (Lee et al., 2001; Wersinger and Sidhu, 2005; Oaks and Sidhu, 2013) and D_2 DA receptor (D_2R; Lee et al., 2007) were thereafter investigated.

As shown in Fig. 3A, the analysis of whole striatal extracts of sham-injected rats under non-reducing conditions shows a dense band at ~75 kDa, corresponding to the DAT glycosylated monomeric isoform (Afonso-Oramas et al., 2009), and a weak band at ~150 kDa, *i.e.* a molecular weight corresponding to DAT dimer. The immunoblot pattern in AAV-tetON-GFP-injected rats receiving 0.5 and 3 mg/ml DOX and AAV-tetON-GDNF-injected rats receiving 0.03 mg/ml DOX was similar to that of sham-injected rats (Fig. 3A, lines 1, 2 and 3). However, the intensity of the 75 kDa band became weaker in AAV-tetON-GDNF injected rats receiving 0.5 and 3 mg/ml DOX (a decrease of 63.5 ± 8.4% in 0,5 mg/ml DOX with respect to Sham, $p < 0.01$, $F = 10.15$; 74.1 ± 6.7% in 3 mg/ml DOX with respect to Sham, $p < 0.01$, $F = 11.29$), and that at ~150 kDa became more intense (an increase of 123.5 ± 8.1% in 0,5 mg/ml DOX with respect to Sham, $p < 0.01$, $F = 11.46$; 144.9 ± 6.8% in 3 mg/ml DOX with respect to Sham, $p < 0.01$, $F = 13.80$), suggesting that prolonged GDNF over-expression enhances the formation of DAT dimers. To confirm this idea, striatal sections of sham-, and AAV-tetON-GFP- and AAV-tetON-GDNF-injected rats treated with 0.5 mg/ml DOX, were processed for DAT–DAT *in situ* PLA using two anti-DAT antibodies against the same DAT epitope domain. Consistent with the suggestion that the ~150 kDa band detected under non-reducing conditions corresponds to DAT dimers, sparse DAT–DAT PLA dots were present around striatal cells in sham and AAV-tetON-GFP-injected rats (Fig. 3B, left), and immunofluoescence for TH confirmed their localization in DA-terminals (Fig. 3B, center and right). The quantitative analysis revealed no differences in the number and size of PLA signals between sham- and AAV-tetON-GFP-injected rats. However, significant differences were found between these two experimental groups and AAV-tetON-GDNF-injected rats (Fig. 3C and D). The number of PLA dots in AAV-tetON-GDNF-injected rats was 81% and 77% higher than in sham ($p < 0.01$ *vs.* sham, $F = 20.64$) and AAV-tetON-GFP-injected rats ($p < 0.01$ *vs.* AAV-tetON-GFP, $F = 20.42$, Fig. 3C) respectively. Likewise, the average dot size in AAV-tetON-GDNF-injected rats (96 ± 7.6 pixels) tripled that of sham- (32 ± 2.3 pixels; $p < 0.001$; $F = 26.78$) and AAV-tetON-GFP-injected rats (34 ± 6.2 pixels; $p < 0.001$; $F = 19.92$; Fig. 3D), with the largest dots probably corresponding to two or more PLA signals localized close to each other. These data together with the differences in the immunoblot pattern

Fig. 1. Striatal GDNF expression. (A) GDNF protein levels (pg/mg protein) measured by ELISA in rat striata 5 weeks after PBS (sham) or viral vector (AAV-tetON-GFP or AAV-tetON-GDNF) injection. Viral vector injected rats were treated with different doses of DOX (0.01, 0.03, 0.5 or 3 mg/ml) in the drinking water. The striatal GDNF levels in AAV-tetON-GDNF injected rats receiving 0.5 mg/ml DOX were 3 times higher than in sham rats and AAV-tetON-GFP-injected rats receiving 0.01 and 3 mg/ml DOX. In AAV-tetON-GDNF injected rats receiving 3 mg/ml DOX, GDNF levels were 12 times higher than in sham and AAV-tetON-GFP-injected rats. (B–I) Immunohistochemistry for GDNF in the striatum of sham rats (B) and viral vector injected rats treated with 0.5 (F) and 3 mg/ml DOX (D, H). (C, E, G and I) High-power magnification microphotographs of B, D, F and H, respectively. GDNF staining was not detected in the striatum of sham rats (C) and AAV-tetON-GFP-injected rats treated with 3 mg/ml DOX (E). Sparse GDNF positive cells were detected in the striatum of AAV-tetON-GDNF-injected rats treated with 0.5 mg/ml DOX (G). Striatal tissue was intensely immunoreactive for GDNF in AAV-tetON-GDNF-injected rats treated with 3 mg/ml DOX (H, I). Scale bar in H (for B, D, F and H), 800 μm; in I (for C, E, G and H), 50 μm.

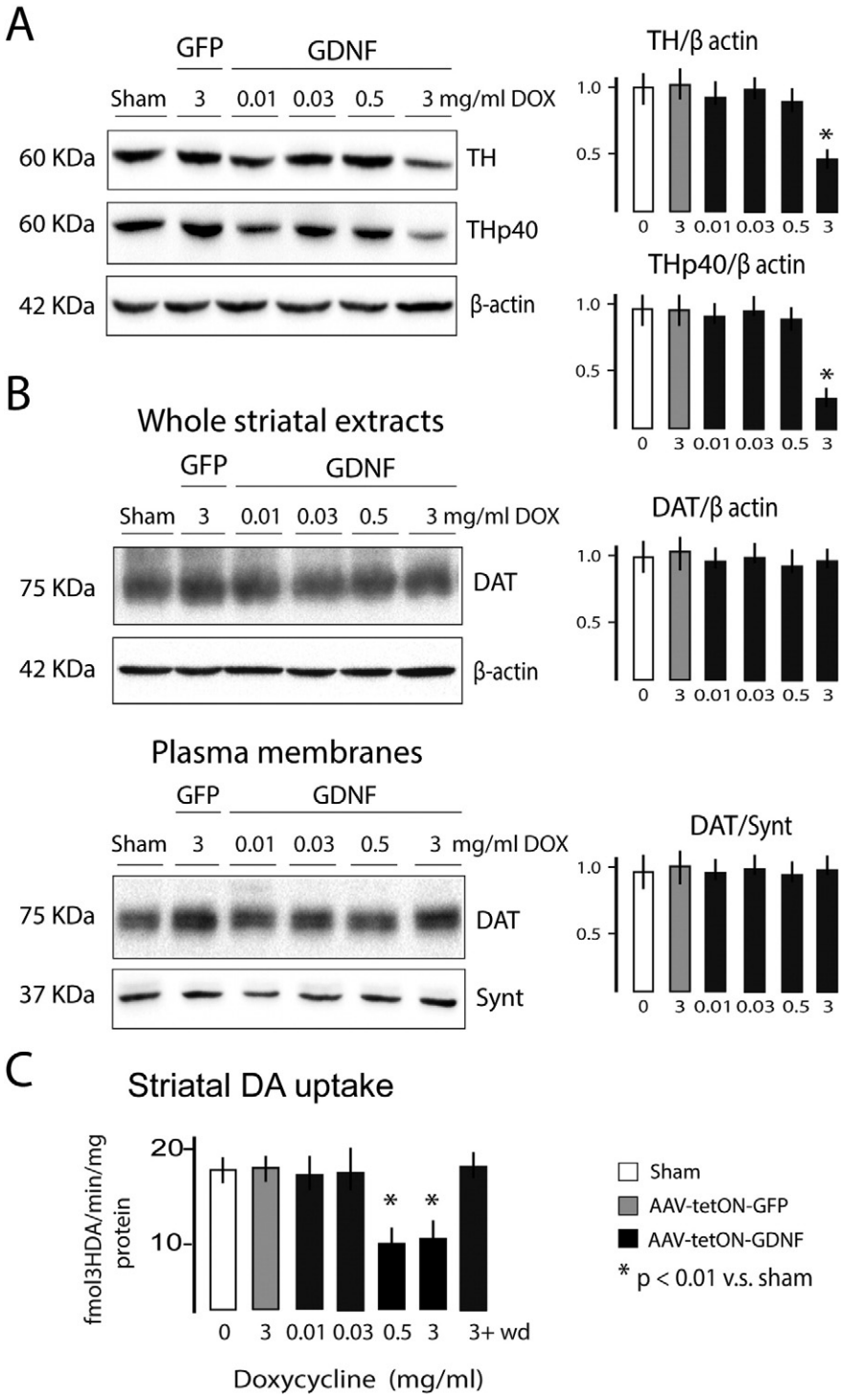

Fig. 2. (A) Western-blot for native TH (TH) and TH phosphorylated at serine 40 (THp40) in whole striatal extracts. (B) Western-blot for DAT in whole striatal extracts and plasma membranes of striatal synaptosomes. (C) Striatal DA uptake. Both TH and THp40 were decreased in the striatum of AAV-tetON-GDNF injected rats treated with 3 mg/ml DOX. No differences were found in the total and membrane DAT levels between sham rats and viral vector injected rats treated with different DOX doses. However, the striatal DA uptake was significantly reduced in AAV-tetON-GDNF injected rats receiving 0.5 and 3 mg/ml DOX, returning to normal levels after 20 days without DOX. β-act, β-actin; synt, syntaxin.

between AAV-tetON-GFP- and AAV-tetON-GDNF-injected rats support the idea that prolonged GDNF over-expression induces DAT dimer formation.

With respect to DAT–α-synuclein and DAT–D_2R interactions, co-immunoprecipitation and *in situ* PLA corroborated previous reports (Lee et al., 2001; Wersinger and Sidhu, 2003; Lee et al., 2007) showing that DAT constitutively maintains a physical interaction with both of them (Fig. 4A–C). However, the response of these interactions to prolonged GDNF over-expression was different. In the case of DAT–α-synuclein, the amount of α-synuclein immunoprecipitated with DAT as well as the number and size of DAT–α-synuclein PLA dots in AAV-tetON-GDNF-injected rats were higher than in AAV-tetON-GFP-injected rats (Fig. 4A, B), suggesting that GDNF over-expression promotes DAT–α-synuclein interaction. In the case of DAT–D_2R, both co-immunoprecipitation and quantitative PLA parameters showed no significant differences between both experimental groups (Fig. 4C, D).

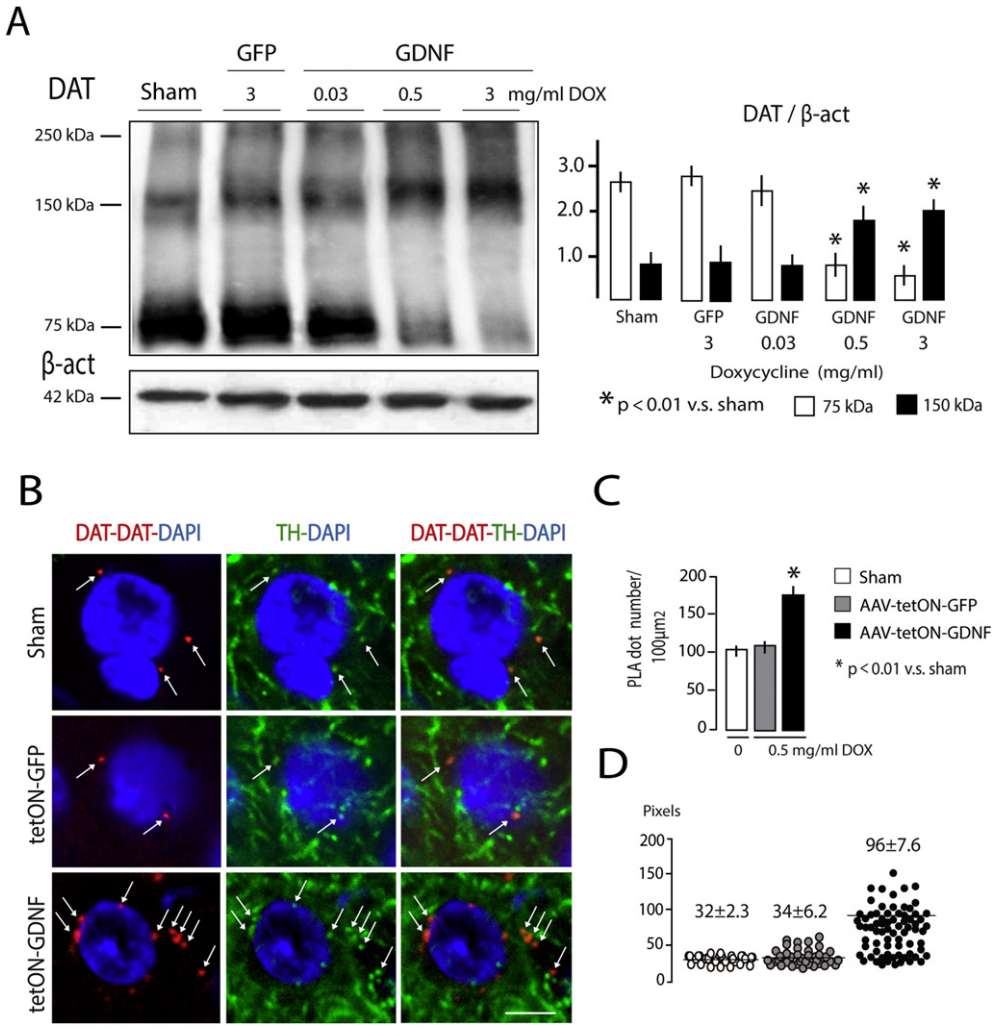

Fig. 3. Effects of GDNF over-expression on DAT–DAT interaction. (A) Western-blot under non-reducing conditions revealed a weak band at 150 kDa, besides that at 75 kDa, in the striatum of sham rats (lane 1), AAV-tetON-GFP-injected rats treated with 3 mg/ml DOX (lane 2), and AAV-tetON-GDNF-injected rats treated with 0.03 mg/ml DOX (lane 3). The high weight band was significantly more intense in labeling and that at 75 kDa became weaker in AAV-tetON-GDNF-injected rats receiving 0.5 and 3 mg/ml DOX (lanes 4 and 5) compared with sham rats ($p < 0.01$). (B) DAT–DAT *in situ* proximity ligation assay (PLA, left) combined with TH immunofluorescence (center) in the striatum of sham rats and viral vector-injected rats treated with 0.5 mg/ml DOX. The quantitative analysis (on the right) showed an increase in both number (top) and size (bottom) of PLA dots in AAV-tetON-GDNF-injected rats treated with 0.5 mg/ml DOX compared with sham rats and AAV-tetON-GFP-injected rats treated with 0.5 mg/ml DOX (C and D; $p < 0.01$). Arrows indicate that DAT–DAT PLA signals (red) localize in DA-terminals (green). Quantitative analysis was performed in 5 animals per group (see the Material and methods section). In the size diagram, the numbers indicate the average size (pixels) of PLA signals. Each dot corresponds to 8 PLA signals in a field of 200 μm^2 from a representative animal. β-act, β-actin. Scale bar in B, 5 μm.

4. Discussion

In sum, our results show that prolonged 12× basal GDNF over-expression induces both DA uptake decrease and TH down-regulation, while 3× basal GDNF over-expression induces DA uptake decrease but not TH down-regulation. The decrease in DA uptake was associated with the formation of DAT dimers and changes in DAT–α-synuclein interaction but not in DAT expression levels or its compartmental distribution.

Tyrosine hydroxylase and DAT, which are responsible for the synthesis and uptake of DA respectively, are pivotal players in DA signaling. Thus, potential antiparkinsonian therapies should preserve TH activity to maintain DA synthesis, but if possible, also regulate DAT activity to maintain DA inputs on postsynaptic receptors and to reduce oxidative stress in surviving neurons. The fact that TH is down-regulated following chronic release of GDNF in rodents (Rosenblad et al., 2003; Georgievska et al., 2004), suggests that other actors in DA handling, *e.g.*, DAT, may be involved in the adaptive response induced by prolonged GDNF transduction. Consistent with this idea, previous studies have shown an inverse relationship between GDNF and DAT expressions. For example, DAT activity is exacerbated in the striatum of GDNF heterozygous mice (Boger et al., 2007; Littrell et al., 2012). In addition, data from our group show that constitutive GDNF mRNA levels in the ventral striatum are higher than in the dorsal striatum, while DAT protein levels and activity are higher in the dorsal striatum than in the ventral striatum (Barroso-Chinea et al., 2005; Afonso-Oramas et al., 2009). In this respect, Zhu et al. (2015) have recently showed that the Rho-family guanine nucleotide exchange factor protein Vav2 interacts with the GDNF receptor tyrosine kinase Ret, forming a functional complex that downregulates DAT activity. Interestingly, Vav2 is robustly expressed in the ventral striatum but not in the dorsal striatum (Zhu et al., 2015), suggesting that the Vav2–Ret interaction may be involved in the differential regulation and functional meaning of DAT between dorsal and ventral striata.

By using intrastriatal injection of an AAV-tetON-GDNF vector and DOX treatment in a dose range of 0.01–3 mg/ml in drinking water, here we show that chronic GDNF release promotes a decrease in DAT activity at an expression level (3× basal levels) lower than that required for TH down-regulation (12× basal levels). We have to note that although the catalytic activity of TH was not directly quantified, the close relationship between Ser40 phosphorylation and TH activity (Dunkley et al., 2004; Daubner et al., 2011; Dickson and Briggs, 2013)

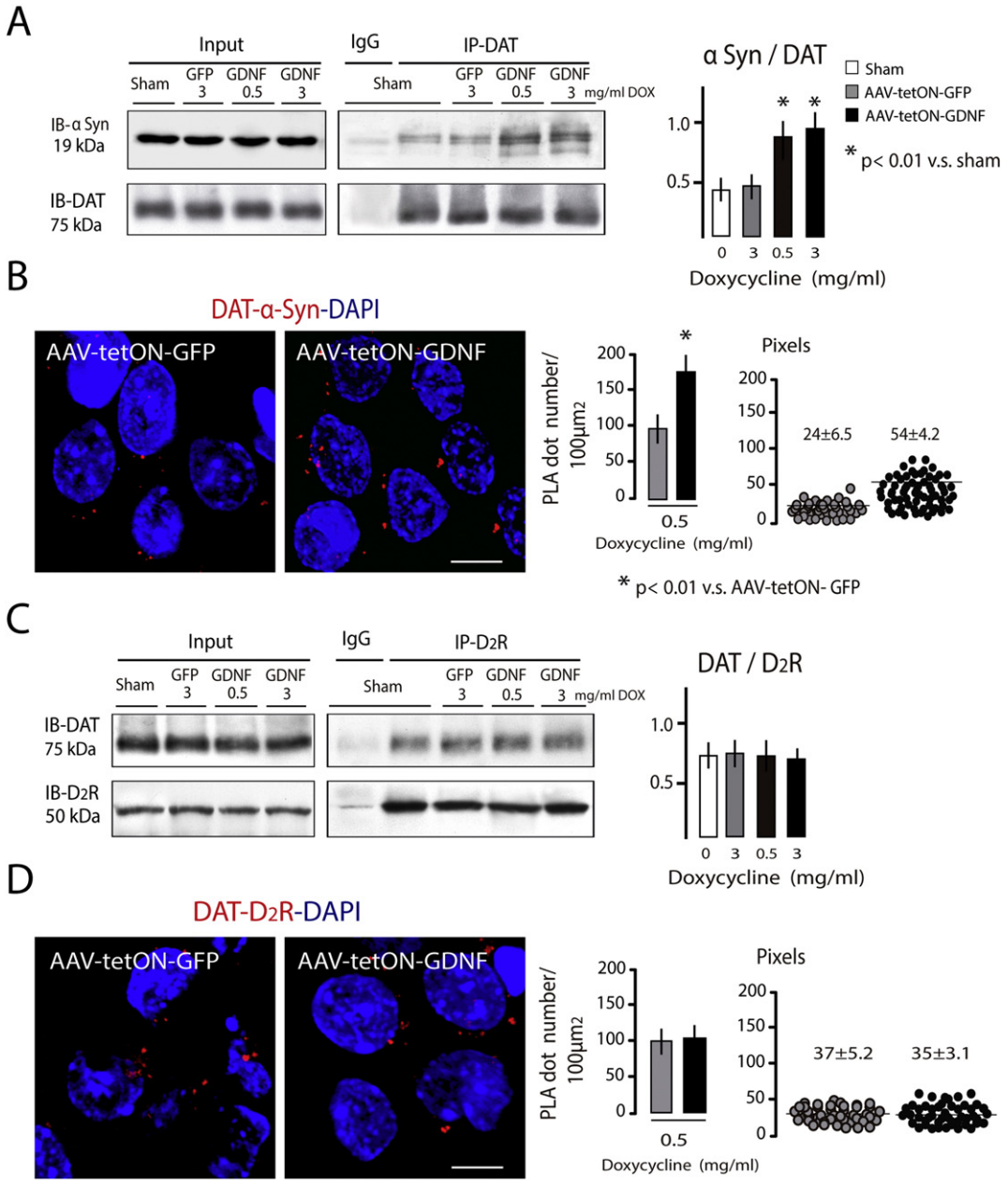

Fig. 4. GDNF over-expression modifies DAT–α synuclein but not DAT–D_2R interaction. (A) Immunoprecipitation for DAT (IP-DAT) and immunoblotting for α-synuclein (IB-α Syn) and DAT (IB-DAT). The quantity of co-immunoprecipitated α-synuclein was higher in AAV-tetON-GDNF-injected DOX (0.5 and 3 mg/ml)-treated rats (lanes 4 and 5) than in sham rats and AAV-tetON-GFP-injected DOX (3 mg/ml)-treated rats (lanes 2 and 3; $p < 0.01$). Lane 1 (IgG), control immunoprecipitation using non-immune IgG. (B) PLA for DAT and α-synuclein in the striatum of AAV-tetON-GFP-injected rats (left) and AAV-tetON-GDNF-injected rats (right) treated with 0.5 mg/ml DOX. The PLA analysis showed that GDNF over-expression increases the number and size of PLA dots ($p < 0.01$ *vs.* AAV-tetON-GFP). (C) Immunoprecipitation for D_2R (IP-D_2R) and immunoblotting for DAT (IB-DAT) and D_2R (IB-D_2R). (D) PLA for DAT and D_2R in the striatum. No differences were found in the levels of co-immunoprecipitated DAT among sham rats and AAV-tetON-GFP- and AAV-tetON-GDNF-injected DOX-treated rats, and in the PLA analysis between both viral vector-injected DOX-treated rats. In (B and D), $n = 5$ animals/group, the numbers in the size diagram indicate the average size (pixels) of PLA signals. Each dot corresponds to 8 PLA signals in a field of 200 μm^2 from a representative animal. Scale bar in B and D, 5 µm.

allows us to assume that TH activity is preserved in AAV-tetON-GDNF-injected rats receiving 0.5 mg/ml DOX.

A large body of evidence indicates that conventional DAT regulation involves protein internalization for it to be thereafter recycled back to the plasma membrane or degraded through the autophagy lysosome pathway (Miranda and Sorkin, 2007; Eriksen et al., 2010a). However, the decline in DA uptake found here after 0.5 mg/ml (3× GDNF basal levels) or 3 mg/ml DOX (12× GDNF basal levels) was not associated with changes in the total expression or compartmental distribution of DAT. Noteworthy, the increase in DA uptake in mice with partial GDNF gene delection is also not paralleled by changes in DAT expression (Boger et al., 2007). Thus, DA uptake may be down- or up-regulated by prolonged GDNF over- or under-expression respectively, without affecting the total DAT expression or its subcellular distribution, suggesting the participation of alternative mechanisms. An increasing number of protein–protein interactions have showed to be involved in DAT trafficking and its recruitment at the plasma membrane (Eriksen et al., 2010b), with some of them, *i.e.* DAT–DAT, DAT–D_2R and DAT–α-synuclein, playing a critical role in DAT function (Hastrup et al., 2001; Wersinger and Sidhu, 2005; Lee et al., 2007; Oaks and Sidhu, 2013). Using western-blot under non-reducing conditions, co-immunoprecipitation and *in situ* PLA, here we show that the decrease in DA uptake following prolonged GDNF release is paralleled by an increase in DAT dimerization and DAT–α-synuclein interaction. In this regard, we have also recently

found that prolonged treatment with the preferential D_3R agonist pramipexole promotes a decrease in DA uptake mediated by changes in DAT interactions with its proteome partners (Castro-Hernández et al., 2015). Thus, changes in DAT–protein interactions may act as adaptive mechanisms of DA-neurons to regulate DA uptake in response to different long-term stimuli. Interestingly, while DAT dimerization is enhanced after prolonged exposition to both pramipexole and GDNF, DAT–D_2R interaction is modified by pramipexole but not by GDNF, and DAT–α-synuclein interaction is strongly modified by GDNF but not by pramipexole. Thus, although further studies involving other DAT interactions are needed, the results suggest that some of them, *i.e.* DAT–DAT, may be sensitive to different conditions, while others, *i.e.* DAT–D_2R and DAT–α-synuclein, respond to specific ones.

Studies in rodents and heterologous expression systems indicate that DAT and other members of the sodium symporter family, such as norepinephrine and serotonin transporters, are assembled as homodimers in the endoplasmic reticulum, and that dimerization is required for their trafficking to the plasma membrane (Kilic and Rudnick, 2000; Hastrup et al., 2001; Torres et al., 2003). In addition, different degrees of oligomerization can coexist in a single cell independently of the transporter density at the plasma membrane (Anderluh et al., 2014). However, the functional meaning of oligomeric forms in the physiology, pathophysiology and pharmacology of transporters has not been elucidated. Consistent with previous studies using western-blot under non-reducing conditions (Baucum et al., 2004; Hadlock et al., 2009), most striatal DAT in sham-treated rats is monomeric (75 kDa), with only a small DAT amount showing a molecular weight that corresponds to the dimeric form (~150 kDa). The inversion of this immunolabeling pattern, consisting in an increase in labeling intensity at 150 kDa and a decrease in that at 75 kDa, observed after prolonged GDNF over-expression suggests a strengthening of DAT–DAT interactions. Similar changes in the DAT expression pattern were found, together with a DA uptake decline, after prolonged treatment with pramipexole (Castro-Hernández et al., 2015) and repeated injections of methamphetamine (Baucum et al., 2004), suggesting a role of DAT dimerization in DA uptake regulation. The evidence of DAT–DAT PLA signals and the increase of them after GDNF over-expression confirm that the 150 kDa band corresponds, at least in part, to DAT dimers. Both the number and the average size of DAT–DAT PLA dots increased after GDNF treatment. The quantitative analysis of PLA signals is currently based on dot count, with the dot number being considered an index of the number of protein–protein interactions (Aubele et al., 2010; Aranguren et al., 2013), while the meaning of dot size has not been clarified. The increase in dot size observed in this study might reflect the presence of two or more PLA signals localized close to each other or the formation of higher order DAT–DAT oligomeric forms. However, until direct evidence provides a solid explanation of this phenomenon we must be cautious in its interpretation.

Alpha-synuclein is a presynaptic protein whose functions have not been entirely clarified. The interest in the role of α-synuclein in DA homeostasis comes from the finding of α-synuclein accumulation in Lewy bodies in parkinsonian brains (Baba et al., 1998), and mutations in the α-synuclein gene in familiar forms of PD (Polymeropoulos et al., 1997). Alpha-synuclein has been involved in the synthesis, vesicular storage and uptake of DA (Perez et al., 2002; Wersinger and Sidhu, 2005). A direct DAT–α-synuclein interaction was identified for the first time by Lee et al. (2001), and thereafter confirmed by other authors (Wersinger and Sidhu, 2003). This interaction can operate at different stages of DAT maturation, including its release from the endoplasmic reticulum, trafficking through cytoskeleton, and recruitment at the plasma membrane (Jeannotte and Sidhu, 2007; Colla et al., 2012; Oaks et al., 2013). Current data indicate that, in contrast to that occurring in α-synuclein over-expression or mutation (Polymeropoulos et al., 1997; Bennett, 2005; Sulzer, 2010), under physiological conditions α-synuclein has a protective effect on DA-neurons. Furthermore, this effect is mediated by its interaction with DAT which acts as a negative modulator in DAT maturation and trafficking, impeding DAT insertion in the plasma membrane, the uptake of DA, and consequently, reducing the oxidative burden in DA-cells (Oaks and Sidhu, 2013). In this context, the finding of an increase in DAT–α-synuclein co-immunoprecipitation and PLA signals, without changes in total α-synuclein levels, indicates that GDNF promotes this interaction as a long-term adaptive mechanism, contributing to the DA uptake decrease and probably to its protective effect on DA-cells.

In conclusion, the use of adeno-associated regulatable vectors and exogenous drugs in a dose-dependent manner allows us to find a point of human GDNF gene transduction at which DAT, but not TH, is regulated. The fact that DA uptake is more sensitive to prolonged GDNF delivery than DA synthesis indicates that at appropriate GDNF transduction levels, DA uptake, and consequently the oxidative burden in DA-cells, may be reduced without interfering with DA synthesis, preventing long-term side effects related to transgene over-expression. This fact may be of interest in the outcome of GDNF in treatment of PD.

Conflict of interest

The authors declare no conflict of interest.

Acknowledgments

This study was supported by the following grants: BFU2010-21130 and BFU2013-47242-R (Ministerio de Ciencia e Innovación, Spain) to TG-H, the Swiss National Research Foundation (FNS; grant number: FN31003A-127177) and EU FP7 Marie Curie IAPP BrainVectors (contract n°. 286071) to L-T; PB-C and JS-H were supported by the IMBRAIN project (FP7-REGPOT-2012-CT2012-31637-IMBRAIN), funded under the 7th Framework Programme (Capacities). JC-H was supported by a predoctoral fellowship from the Fundación Canaria de Investigación y Salud (ID54). The authors thank Catherine Pythoud for her excellent technical assistance in vector preparation.

References

Afonso-Oramas, D., Cruz-Muros, I., Alvarez de la Rosa, D., Abreu, P., Giraldez, T., Castro-Hernández, J., Salas-Hernández, J., Lanciego, J.L., Rodríguez, M., González-Hernández, T., 2009. Dopamine transporter glycosylation correlates with the vulnerability of midbrain dopaminergic cells in Parkinson's disease. Neurobiol. Dis. 36, 494–508. http://dx.doi.org/10.1016/j.nbd.2009.09.002.

Afonso-Oramas, D., Cruz-Muros, I., Barroso-Chinea, P., Álvarez de la Rosa, D., Castro-Hernández, J., Salas-Hernández, J., Giráltez, T., González-Hernández, T., 2010. The dopamine transporter is differentially regulated after dopaminergic lesion. Neurobiol. Dis. 40, 518–530. http://dx.doi.org/10.1016/j.nbd.2010.07.012.

Alexi, T., Borlongan, C.V., Faull, R.L., Williams, C.E., Clark, R.G., Gluckman, P.D., Hughes, P.E., 2000. Neuroprotective strategies for basal ganglia degeneration: Parkinson's and Huntington's diseases. Prog. Neurobiol. 60, 409–470. http://dx.doi.org/10.1016/S0301-0082(99)00032-5.

Anderluh, A., Klotzsch, E., Reismann, A.W., Brameshuber, M., Kudlacek, O., Newman, A.H., Sitte, H.H., Schütz, G.J., 2014. Single molecule analysis reveals coexistence of stable serotonin transporter monomers and oligomers in the live cell plasma membrane. J. Biol. Chem. 289, 4387–4394. http://dx.doi.org/10.1074/jbc.M113.531632.

Apawu, A.K., Maina, F.K., Taylor, J.R., Mathews, T.A., 2013. Probing the ability of presynaptic tyrosine kinase receptors to regulate striatal dopamine dynamics. ACS Chem. Neurosci. 4, 895–904. http://dx.doi.org/10.1021/cn4000742.

Aranguren, X.L., Beerens, M., Coppiello, G., Wiese, C., Vandersmissen, I., Lo Nigro, A., Verfaillie, C.M., Gessler, M., Luttun, A., 2013. COUP-TFII orchestrates venous and lymphatic endothelial identity by homo- or hetero-dimerisation with PROX1. J. Cell Sci. 126, 1164–1175. http://dx.doi.org/10.1242/jcs.116293.

Aubele, M., Spears, M., Ludyga, N., Braselmann, H., Feuchtinger, A., Taylor, K.J., Lindner, K., Auer, G., Stering, K., Höfler, H., Schmitt, M., Bartlett, J.M., 2010. In situ quantification of HER2-protein tyrosine kinase 6 (PTK6) protein–protein complexes in paraffin sections from breast cancer tissues. Br. J. Cancer 103, 663–667. http://dx.doi.org/10.1038/sj.bjc.6605836.

Baba, M., Nakajo, S., Tu, P.H., Tomita, T., Nakaya, K., Lee, V.M., Trojanowski, J.Q., Iwatsubo, T., 1998. Aggregation of alpha-synuclein in Lewy bodies of sporadic Parkinson's disease and dementia with Lewy bodies. Am. J. Pathol. 152, 879–884.

Bannon, M.J., 2005. The dopamine transporter: role in neurotoxicity and human disease. Toxicol. Appl. Pharmacol. 204, 355–360. http://dx.doi.org/10.1016/j.taap.2004.08.013.

Barroso-Chinea, P., Cruz-Muros, I., Aymerich, M.S., Rodriguez-Diaz, M., Afonso-Oramas, D., Lanciego, J.L., Gonzalez-Hernandez, T., 2005. Striatal expression of GDNF and

differential vulnerability of midbrain dopaminergic cells. Eur. J. Neurosci. 21, 1815–1827. http://dx.doi.org/10.1111/j.1460-9568.2005.04024.x.
Baucum II, A.J., Rau, K.S., Riddle, E.L., Hanson, G.R., Fleckenstein, A.E., 2004. Methamphetamine increases dopamine transporter higher molecular weight complex formation via a dopamine- and hyperthermia-associated mechanism. J. Neurosci. 24, 3436–3443. http://dx.doi.org/10.1523/JNEUROSCI. 0387–04.2004.
Bennett, M.C., 2005. The role of alpha-synuclein in neurodegenerative diseases. Pharmacol. Ther. 105, 311–331. http://dx.doi.org/10.1016/j.pharmthera.2004.10.010.
Bezard, E., Gross, C.E., Fournier, M.C., Dovero, S., Bloch, B., Jaber, M., 1999. Absence of MPTP-induced neuronal death in mice lacking the dopamine transporter. Exp. Neurol. 155, 268–273. http://dx.doi.org/10.1006/exnr.1998.6995.
Boger, H.A., Middaugh, L.D., Patrick, K.S., Ramamoorthy, S., Denehy, E.D., Zhu, H., Pacchioni, A.M., Granholm, A.C., McGinty, J.F., 2007. Long-term consequences of methamphetamine exposure in young adults are exacerbated in glial cell line-derived neurotrophic factor heterozygous mice. J. Neurosci. 27, 8816–8825. http://dx.doi.org/10.1523/JNEUROSCI.1067-07.2007.
Castro-Hernández, J., Afonso-Oramas, D., Cruz-Muros, I., Salas-Hernández, J., Barroso-Chinea, P., Rosario Moratalla, R., Millan, M.J., González-Hernández, T., 2015. Prolonged treatment with pramipexole promotes physical interaction of striatal dopamine D3 autoreceptors with dopamine transporters to reduce dopamine uptake. Neurobiol. Dis. 74, 325–335. http://dx.doi.org/10.1016/j.nbd.2014.12.007.
Chen, N., Reith, M.E., 2008. Substrates dissociate dopamine transporter oligomers. J. Neurochem. 105, 910–920. http://dx.doi.org/10.1111/j.1471-4159.2007.05195.x.
Chtarto, A., Bockstael, O., Tshibangu, T., Dewitte, O., Levivier, M., Tenenbaum, L., 2013. A next step in adeno-associated virus (AAV)-mediated gene therapy for neurological diseases: regulation and targeting. Br. J. Clin. Pharmacol. 76, 217–232. http://dx.doi.org/10.1111/bcp.12065.
Chtarto, A., Yang, X., Bockstael, O., Melas, C., Blum, D., Lehtonen, E., Abeloos, L., Jaspar, J.M., Levivier, M., Brotchi, J., Velu, T., Tenenbaum, L., 2007. Controlled delivery of glial cell line-derived neurotrophic factor by a single tetracycline-inducible AAV vector. Exp. Neurol. 204, 387–399. http://dx.doi.org/10.1016/j.expneurol.2006.11.014.
Colla, E., Jensen, P.H., Pletnikova, O., Troncoso, J.C., Glabe, C., Lee, M.K., 2012. Accumulation of toxic α-synuclein oligomer within endoplasmic reticulum occurs in α-synucleinopathy in vivo. J. Neurosci. 32, 3301–3305. http://dx.doi.org/10.1523/JNEUROSCI.5368-11.2012.
Cruz-Muros, I., Afonso-Oramas, D., Abreu, P., Perez-Delgado, M.M., Rodriguez, M., Gonzalez-Hernandez, T., 2009. Aging effects on the dopamine transporter expression and compensatory mechanisms. Neurobiol. Aging 30, 973–986. http://dx.doi.org/10.1016/j.neurobiolaging.2007.09.009.
Daubner, S.C., Le, T., Wang, S., 2011. Tyrosine hydroxylase and regulation of dopamine synthesis. Arch. Biochem. Biophys. 508, 1–12. http://dx.doi.org/10.1016/j.abb.2010.12.017.
Dickson, P.W., Briggs, G.D., 2013. Tyrosine hydroxylase: regulation by feedback inhibition and phosphorylation. Adv. Pharmacol. 68, 13–21. http://dx.doi.org/10.1016/B978-0-12-411512-5.00002-6.
Dunkley, P.R., Bobrovskaya, L., Graham, M.E., von Nagy-Felsobuki, E.I., Dickson, P.W., 2004. Tyrosine hydroxylase phosphorylation: regulation and consequences. J. Neurochem. 91, 1025–1043. http://dx.doi.org/10.1111/j.1471-4159.2004.02797.x.
Eriksen, J., Bjørn-Yoshimoto, W.E., Jørgensen, T.N., Newman, A.H., Gether, U., 2010a. Postendocytic sorting of constitutively internalized dopamine transporter in cell lines and dopaminergic neurons. J. Biol. Chem. 285, 27289–27301. http://dx.doi.org/10.1074/jbc.M110.131003.
Eriksen, J., Jørgensen, T.N., Gether, U., 2010b. Regulation of dopamine transporter function by protein–protein interactions: new discoveries and methodological challenges. J. Neurochem. 113, 27–41. http://dx.doi.org/10.1111/j.1471-4159.2010.06599.x.
Foster, J.D., Yang, J.W., Moritz, A.E., Challasivakanaka, S., Smith, M.A., Holy, M., Wilebski, K., Sitte, H.H., Vaughan, R.A., 2012. Dopamine transporter phosphorylation site threonine 53 regulates substrate reuptake and amphetamine-stimulated efflux. J. Biol. Chem. 287, 29702–29712. http://dx.doi.org/10.1074/jbc.M112.367706.
Freed, C., Revay, R., Vaughan, R.A., Kriek, E., Grant, S., Uhl, G.R., Kuhar, M.J., 1995. Dopamine transporter immunoreactivity in rat brain. J. Comp. Neurol. 359, 340–349. http://dx.doi.org/10.1002/cne.903590211.
Gabriel, L.R., Wu, S., Kearney, P., Bellvé, K.D., Standley, C., Fogarty, K.E., Melikian, H.E., 2013. Dopamine transporter endocytic trafficking in striatal dopaminergic neurons: differential dependence on dynamin and the actin cytoskeleton. J. Neurosci. 33, 17836–17846. http://dx.doi.org/10.1523/JNEUROSCI.3284-13.2013.
Garbayo, E., Ansorena, E., Lanciego, J.L., Blanco-Prieto, M.J., Aymerich, M.S., 2011. Long-term neuroprotection and neurorestoration by glial cell-derived neurotrophic factor microspheres for the treatment of Parkinson's disease. Mov. Disord. 26, 1943–1947. http://dx.doi.org/10.1002/mds.23793.
Georgievska, B., Kirik, D., Björklund, A., 2004. Overexpression of glial cell line-derived neurotrophic factor using a lentiviral vector induces time- and dose-dependent downregulation of tyrosine hydroxylase in the intact nigrostriatal dopamine system. J. Neurosci. 24, 6437–6445. http://dx.doi.org/10.1523/JNEUROSCI.1122-04.2004.
Giros, B., Caron, M.G., 1993. Molecular characterization of the dopamine transporter. Trends Pharmacol. Sci. 14, 43–49. http://dx.doi.org/10.1016/0165-6147(93)90029-J.
Giros, B., Jaber, M., Jones, S.R., Wightman, R.M., Caron, M.G., 1996. Hyperlocomotion and indifference to cocaine and amphetamine in mice lacking the dopamine transporter. Nature 379, 606–612. http://dx.doi.org/10.1038/379606a0.
González, M.I., Robinson, M.B., 2004. Neurotransmitter transporters: why dance with so many partners? Curr. Opin. Pharmacol. 4, 30–35. http://dx.doi.org/10.1016/j.coph.2003.09.004.
Gonzalez-Hernandez, T., Barroso-Chinea, P., de la Cruz-Muros, I., Pérez-Delgado, M.M., Rodríguez, M., 2004. Expression of dopamine and vesicular monoamine transporters and differential vulnerability of mesostriatal dopaminergic neurons. J. Comp. Neurol. 479, 198–215. http://dx.doi.org/10.1002/cne.20323.
Goverdhana, S., Puntel, M., Xiong, W., Zirger, J.M., Barcia, C., Curtin, J.F., Soffer, E.B., Mondkar, S., King, G.D., Hu, J., Sciascia, S.A., Candolfi, M., Greengold, D.S., Lowenstein, P.R., Castro, M.G., 2005. Regulatable gene expression systems for gene therapy applications: progress and future challenges. Mol. Ther. 12, 189–211. http://dx.doi.org/10.1016/j.ymthe.2005.03.022.
Hadlock, G.C., Baucum II, A.J., King, J.L., Horner, K.A., Cook, G.A., Gibb, J.W., Wilkins, D.G., Hanson, G.R., Fleckenstein, A.E., 2009. Mechanisms underlying methamphetamine-induced dopamine transporter complex formation. J. Pharmacol. Exp. Ther. 329, 169–174. http://dx.doi.org/10.1124/jpet.108.145631.
Hadlock, G.C., Nelson, C.C., Baucum II, A.J., Hanson, G.R., Fleckenstein, A.E., 2011. Ex vivo identification of protein–protein interactions involving the dopamine transporter. J. Neurosci. Methods 196, 303–307. http://dx.doi.org/10.1016/j.jneumeth.2011.01.023.
Hastrup, H., Karlin, A., Javitch, J.A., 2001. Symmetrical dimer of the human dopamine transporter revealed by cross-linking Cys-306 at the extracellular end of the sixth transmembrane segment. Proc. Natl. Acad. Sci. U. S. A. 98, 10055–10060. http://dx.doi.org/10.1073/pnas.181344298.
Jeannotte, A.M., Sidhu, A., 2007. Regulation of the norepinephrine transporter by alpha-synuclein-mediated interactions with microtubules. Eur. J. Neurosci. 26, 1509–1520. http://dx.doi.org/10.1111/j.1460-9568.2007.05757.x.
Kilic, F., Rudnick, G., 2000. Oligomerization of serotonin transporter and its functional consequences. Proc. Natl. Acad. Sci. U. S. A. 97, 3106–3111. http://dx.doi.org/10.1073/pnas.97.7.3106.
Kirik, D., Georgievska, B., Bjorklund, A., 2004. Localized striatal delivery of GDNF as a treatment for Parkinson disease. Nat. Neurosci. 7, 105–110. http://dx.doi.org/10.1038/nn1175nn1175.
Le Couteur, D.G., Leighton, P.W., McCann, S.J., Pond, S.M., 1997. Association of a polymorphism in the dopamine-transporter gene with Parkinson's disease. Mov. Disord. 12, 760–763. http://dx.doi.org/10.1002/mds.870120523.
Lee, F.J.S., Liu, F., Pristupa, Z.B., Niznik, H.B., 2001. Direct binding and functional coupling of alpha-synuclein to the dopamine transporters accelerate dopamine-induced apoptosis. FASEB J. 15, 916–926. http://dx.doi.org/10.1096/fj.00-0334com.
Lee, F.J.S., Pei, L., Moszczynska, A., Vukusic, B., Fletcher, P.J., Liu, F., 2007. Dopamine transporter cell surface localization facilitated by a direct interaction with the dopamine D2 receptor. EMBO J. 26, 2127–2136. http://dx.doi.org/10.1038/sj.emboj.7601656.
Lin, L.F., Doherty, D.H., Lile, J.D., Bektesh, S., Collins, F., 1993. GDNF: a glial cell line-derived neurotrophic factor for midbrain dopaminergic neurons. Science 260, 1130–1132. http://dx.doi.org/10.1126/science.8493557.
Littrell, O.M., Pomerleau, F., Huettl, P., Surgener, S., McGinty, J.F., Middaugh, L.D., Granholm, A.C., Gerhardt, G.A., Boger, H.A., 2012. Enhanced dopamine transporter activity in middle-aged Gdnf heterozygous mice. Neurobiol. Aging 33 (427), e1–14. http://dx.doi.org/10.1016/j.neurobiolaging.2010.10.013.
Lock, M., McGorray, S., Auricchio, A., Ayuso, E., Beecham, E.J., Blouin-Tavel, V., Bosch, F., Bose, M., Byrne, B.J., Caton, T., Chiorini, J.A., Chtarto, A., Clark, K.R., Conlon, T., Darmon, C., Doria, M., Douar, A., Flotte, T.R., Francis, J.D., Francois, A., Giacca, M., Korn, M.T., Korytov, I., Leon, X., Leuchs, B., Lux, G., Melas, C., Mizukami, H., Moullier, P., Müller, M., Ozawa, K., Philipsberg, T., Poulard, K., Raupp, C., Rivière, C., Roosendaal, S.D., Samulski, R.J., Soltys, S.M., Surosky, R., Tenenbaum, L., Thomas, D.L., Van Montfort, B., Veres, G., Wright, J.F., Xu, Y., Zelenaia, O., Zentilin, L., Snyder, R.O., 2010. Characterization of a recombinant adeno-associated virus type 2 reference standard material. Hum. Gene Ther. 21, 1273–1285. http://dx.doi.org/10.1089/hum.2009.223.
Miranda, M., Sorkin, A., 2007. Regulation of receptors and transporters by ubiquitination: new insights into surprisingly similar mechanisms. Mol. Interv. 7, 157–167. http://dx.doi.org/10.1124/mi.7.3.7.
Mortensen, O.V., Amara, S.G., 2003. Dynamic regulation of the dopamine transporter. Eur. J. Pharmacol. 479, 159–170. http://dx.doi.org/10.1016/j.ejphar.2003.08.066.
Oaks, A.W., Sidhu, A., 2013. Parallel mechanisms for direct and indirect membrane protein trafficking by synucleins. Commun. Integr. Biol. 6, e26794. http://dx.doi.org/10.4161/cib.26794.
Oaks, A.W., Marsh-Armstrong, N., Jones, J.M., Credle, J.J., Sidhu, A., 2013. Synucleins antagonize endoplasmic reticulum function to modulate dopamine transporter trafficking. PLoS ONE 8, e70872. http://dx.doi.org/10.1371/journal.pone.0070872.
Pascual, A., Hidalgo-Figueroa, M., Piruat, J.I., Pintado, C.O., Gomez-Diaz, R., Lopez-Barneo, J., 2008. Absolute requirement of GDNF for adult catecholaminergic neuron survival. Nat. Neurosci. 11, 755–761. http://dx.doi.org/10.1038/nn.2136.
Paxinos, G., Watson, C., 1998. The Rat Brain in Stereotaxic Coordinates. Academic Press, Orlando.
Perez, R.G., Waymire, J.C., Lin, E., Liu, J.J., Guo, F., Zigmond, M.J., 2002. A role for alpha-synuclein in the regulation of dopamine biosynthesis. J. Neurosci. 22, 3090–3099 (DOI: 11943812).
Polymeropoulos, M.H., Lavedan, C., Leroy, E., Ide, S.E., Dehejia, A., Dutra, A., Pike, B., Root, H., Rubenstein, J., Boyer, R., Stenroos, E.S., Chandrasekharappa, S., Athanassiadou, A., Papapetropoulos, T., Johnson, W.G., Lazzarini, A.M., Duvoisin, R.C., Di Iorio, G., Golbe, L.I., Nussbaum, R.L., 1997. Mutation in the alpha-synuclein gene identified in families with Parkinson's disease. Science 276, 2045–2047. http://dx.doi.org/10.1126/science.276.5321.2045.
Rosenblad, C., Georgievska, B., Kirik, D., 2003. Long-term striatal overexpression of GDNF selectively downregulates tyrosine hydroxylase in the intact nigrostriatal dopamine system. Eur. J. Neurosci. 17, 260–270. http://dx.doi.org/10.1046/j.1460-9568.2003.02456.x.
Sajadi, A., Bauer, M., Thöny, B., Aebischer, P., 2005. Long-term glial cell line-derived neurotrophic factor overexpression in the intact nigrostriatal system in rats leads to a decrease of dopamine and increase of tetrahydrobiopterin production. J. Neurochem. 93, 1482–1486. http://dx.doi.org/10.1111/j.1471-4159.2005.03139.x.
Salvatore, M.F., Apparsundaram, S., Gerhardt, G.A., 2003. Decreased plasma membrane expression of striatal dopamine transporter in aging. Neurobiol. Aging 24, 1147–1154. http://dx.doi.org/10.1016/S0197-4580(03)00129-5.

Salvatore, M.F., Zhang, J.L., Large, D.M., Wilson, P.E., Gash, C.R., Thomas, T.C., Haycock, J.W., Bing, G., Stanford, J.A., Gash, D.M., Gerhardt, G.A., 2004. Striatal GDNF administration increases tyrosine hydroxylase phosphorylation in the rat striatum and substantia nigra. J. Neurochem. 90, 245–254. http://dx.doi.org/10.1111/j.1471-4159.2004.02496.x.

Schober, A., 2004. Classic toxin-induced animal models of Parkinson's disease: 6-OHDA and MPTP. Cell Tissue Res. 318, 215–224. http://dx.doi.org/10.1007/s00441-004-0938-y.

Söderberg, O., Leuchowius, K.J., Gullberg, M., Jarvius, M., Weibrecht, I., Larsson, L.G., Landegren, U., 2008. Characterizing proteins and their interactions in cells and tissues using the in situ proximity ligation assay. Methods 45, 227–232. http://dx.doi.org/10.1016/j.ymeth.2008.06.014.

Storch, A., Ludolph, A.C., Schwarz, J., 2004. Dopamine transporter: involvement in selective dopaminergic neurotoxicity and degeneration. J. Neural Transm. 111, 1267–1286. http://dx.doi.org/10.1007/s00702-004-0203-2.

Sulzer, D., 2010. Clues to how alpha-synuclein damages neurons in Parkinson's disease. Mov. Disord. 25, S27–S31. http://dx.doi.org/10.1002/mds.22639.

Torres, G.E., Carneiro, A., Seamans, K., Fiorentini, C., Sweeney, A., Yao, W.D., Caron, M.G., 2003. Oligomerization and trafficking of the human dopamine transporter. Mutational analysis identifies critical domains important for the functional expression of the transporter. J. Biol. Chem. 278, 2731–2739. http://dx.doi.org/10.1074/jbc.M201926200.

Uhl, G.R., Walther, D., Mash, D., Faucheux, B., Javoy-Agid, F., 1994. Dopamine transporter messenger RNA in Parkinson's disease and control substantia nigra neurons. Ann. Neurol. 35, 494–498. http://dx.doi.org/10.1002/ana.410350421.

Wersinger, C., Sidhu, A., 2003. Attenuation of dopamine transporter activity by alphasynuclein. Neurosci. Lett. 340, 189–192. http://dx.doi.org/10.1016/S0304-3940(03)00097-1.

Wersinger, C., Sidhu, A., 2005. Disruption of the interaction of alpha-synuclein with microtubules enhances cell surface recruitment of the dopamine transporter. Biochemistry 44, 13612–13624. http://dx.doi.org/10.1021/bi050402p.

Yang, X., Mertens, B., Lehtonen, E., Vercammen, L., Bockstael, O., Chtarto, A., Levivier, M., Brotchi, J., Michotte, Y., Baekelandt, V., Sarre, S., Tenenbaum, L., 2009. Reversible neurochemical changes mediated by delayed intrastriatal glial cell line-derived neurotrophic factor gene delivery in a partial Parkinson's disease rat model. J. Gene Med. 11, 899–912. http://dx.doi.org/10.1002/jgm.1377.

Zahniser, N.R., Sorkin, A., 2009. Trafficking of dopamine transporter in psychostimulant actions. Semin. Cell Dev. Biol. 20, 411–417. http://dx.doi.org/10.1016/j.semcdb.2009.01.004.

Zhou, X., Vink, M., Klaver, B., Berkhout, B., Das, A.T., 2006. Optimization of the Tet-On system for regulated gene expression through viral evolution. Gene Ther. 13, 1382–1390. http://dx.doi.org/10.1038/sj.gt.3302780.

Zhu, S., Zhao, C., Wu, Y., Yang, Q., Shao, A., Wang, T., Wu, J., Yin, Y., Li, Y., Hou, J., Zhang, X., Zhou, G., Gu, X., Wang, X., Bustelo, X.R., Zhou, J., 2015. Identification of a Valv2-dependent mechanism for GDNF/Ret control of mesolimbic DAT trafficking. Nat. Neurosci. 18, 1084–1093. http://dx.doi.org/10.1038/nn.4060.

Zieba, A., Wahlby, C., Hjelm, F., Jordan, L., Berg, J., Landegren, U., Pardali, K., 2010. Bright-field microscopy visualization of proteins and protein complexes by in situ proximity ligation with peroxidase detection. Clin. Chem. 56, 99–110. http://dx.doi.org/10.1373/clinchem.2009.134452.

Zolotukhin, S., Potter, M., Zolotukhin, I., Sakai, Y., Loiler, S., Fraites Jr., T.J., Chiodo, V.A., Phillipsberg, T., Muzyczka, N., Hauswirth, W.W., Flotte, T.R., Byrne, B.J., Snyder, R.O., 2002. Production and purification of serotype 1, 2, and 5 recombinant adeno-associated viral vectors. Methods 28, 158–167. http://dx.doi.org/10.1016/S1046-2023(02)00220-7.